Journal of Undergraduate Research in Physics
August 19, 2010

A New Assessment of Dark Matter in the Milky Way Galaxy

Grant Remmen

August 19, 2010

School of Physics and Astronomy, 116 Church Street S.E.,
College of Science and Engineering, University of Minnesota, Minneapolis, MN, United States
Address for correspondence: 272 Cherry Ridge Drive, Detroit Lakes, MN
E-mail address: remme024@umn.edu

Abstract

Through an examination of recent data on the mass distribution and velocity curve of the Milky Way Galaxy, I produce a new estimate of the dark matter distribution, as well as the overall dark matter content, of our galaxy. Initially, I develop a model of the baryonic mass of the galaxy (i.e. luminous matter and interstellar clouds). This model incorporates three components: an exponential stellar disc and a central stellar bulge, based on the Tuorla–Heidelberg model, and a gaseous layer, fit to the gas density distribution data of Olling & Merrifield (2001). Secondly, incorporating recent data, I calculate an updated rotational velocity curve for the galaxy as a function of galactocentric radius. Using this velocity curve, I determine total galactic mass as a function of radius and compare this with the baryonic mass model to determine the distribution of dark matter in the galaxy, with improved precision and over a greater spatial range than previous estimates. This calculation results in a radial dark matter density distribution that falls off with large distance in a characteristic fashion. Finally, I show that neutrinos, particles that have often been suggested as a component of dark matter, cannot make up more than a very small amount of the galactic dark matter content.

Key Words : Galaxy: kinematics and dynamics, Galaxy: structure, dark matter, neutrinos

1 Introduction

For many years, it has been known that the observed rotation rates of spiral galaxies differ greatly from the rates predicted based on the observable luminous masses of the galaxies. This simple observation has led to the proposition that large amounts of invisible matter, known as dark matter, are distributed within and around these galaxies, accounting for the greater gravity and thus faster rotation than what would be predicted from the luminous mass alone. While this is accepted as fact and the dark matter distribution associated with various cosmic objects has been determined, a point of constant curiosity has been the dark matter distribution within our home galaxy. The following determination of the pattern and content of the dark matter halo within the Milky Way will allow for more decisive and conclusive experimentation in the future, through the detection of particles, such as neutrinos, that have been proposed as candidates to explain the effects of dark matter. Further, the dark matter distribution of the galaxy is of great theoretical interest with regard to the dynamics of our galaxy as it formed and evolved.

In calculating the distribution of the Milky Way's dark matter halo, I assume that the Gaussian approximation for gravity is applicable to the galaxy. Specifically, this means that, for a piece of matter located at a given galactocentric radius, the net gravitational force at that position is equal to the gravitational force due to the mass interior to that radius and acts as though this entire interior mass were concentrated at the center of the galaxy. This approximation is mathematically valid and exact for any spherically symmetric mass distribution, by Gauss' law for gravity, or alternatively by Newton's law of universal gravitation. However, the Gaussian approximation is a commonly used tool in studies of galactic rotation. As shown by Binney & Tremaine (1987), the peak rotational velocity within an exponential disc as compared to the peak velocity within the corresponding spherically distributed body is higher only by approximately 15 percent, while the velocities at large radii differ by only a negligible amount. Furthermore, the galaxy has more of a spherical character than that of a pure exponential disc, as a result of its central stellar bulge. Thus, while the assumption of the applicability of Gauss' law for gravity in this manner may cause the supposition of a bit more dark matter within the interior of the galaxy, the calculation of the total amount of dark matter interior to large radii will not be aversely affected by this method.

Once the supposition of the Gaussian approximation for gravity has been accepted, the calculation of the mass interior to a galactocentric radius, given the circular velocity of matter at that radius, is straightforward. By equating the magnitude of the centripetal acceleration to the gravitational force per unit mass, one may deduce that:

$$M_V(R) = \frac{R\left[V(R)\right]^2}{G}, \tag{1}$$

where $M_V(R)$ denotes the total mass (based on the velocity curve) interior to a galactocentric radius R.

In all calculations, I use the latest (2006) value of $G = 6.67428 \times 10^{-11}$ m^3 kg^{-1} s^{-2}, specified by the Committee on Data for Science and Technology (CODATA) of the International Council for Science and accepted by the National Institute of Standards and Technology (NIST) (Mohr, Taylor & Newell 2007). For an accurate definition of the kiloparsec in units of meters, I use the value from the Explanatory Supplement to the Astronomical Almanac (Seidelmann 2005): 1 kpc = $3.085677582 \times 10^{19}$ m. Finally, for the unit of the solar mass, I use the official value provided by the National Aeronautics and Space Administration (NASA) of 1.989100×10^{30} kg (Williams 2004).

First, however, in Section 2, I shall describe a model for the baryonic mass distribution of the galaxy. This mass model consists of a density function $\rho_{\text{model}}(R)$, which is assumed to be a function of radius only. That is, consistent with the above discussion, the mass of the galaxy is considered to have the form of the equivalent spherically symmetric mass distribution, for the purposes of the Gaussian approximation for the gravitational pull of matter interior to a given galactocentric radius. As will be shown in the following Section, the baryonic mass model for the galaxy has the form

$$\rho_{\text{model}}(R) = \begin{cases} \frac{1}{2R}\Sigma_0 e^{-R/R_{\text{d}}} & \text{disc} \\ \frac{\rho_{\text{bulge},0}}{\eta\zeta b_{\text{m}}^3}\frac{\exp\left[-(R/b_{\text{m}})^2\right]}{(1+R/b_0)^{1.8}} & \text{bulge} \\ \sum_{i=1}^{3}\frac{G_i}{2}R^{i-1} \text{for } R \leq 23.521 \text{ kpc} & \text{interstellar gas} \end{cases}, \tag{2}$$

where the constants for each component are defined in their respective portion of Section 2 (Section 2.1 for the disc, 2.2 for the bulge, and 2.3 for the interstellar gas). As will be demonstrated in Section 2, to find the total baryonic mass interior to a given galactocentric radius, the density function is integrated: $M_{\text{model}}(R) = 4\pi\int_0^R r^2\rho_{\text{model}}(r)\,dr$.

In all final results of calculations (both in text and in Table 5), values are rounded to an appropriate number of significant figures. However, the reader should note that, consistent with previous studies of the velocity curve (e.g. Clemens 1985), I report values of the constants for the curve to a large number of figures to preserve continuity of the curve and reproducibility of the calculation. Since the

velocity curve is a piecewise function, rounding leads to gaps in the curve; these gaps would create difficulties for an interested reader reproducing the calculation or using the model for other purposes. Though the models are robust, it is useful to preserve more digits in intermediate results, so as not to introduce roundoff errors in subsequent calculations. For these reasons, I report the constants for all intermediate calculational steps (velocity curve, baryonic mass model, etc.) to a large number of figures, as in Tables 1 through 4 and Equation 15. Nonetheless, all final quoted results are rounded to significant figures.

2 The Mass Model of the Milky Way Galaxy

The "normal" matter of the Milky Way Galaxy, also known as the baryonic mass, is composed primarily of three components: an exponential disc of stars that thins out dramatically at large distances from the galactic center, a central stellar bulge, and a distribution of atomic and molecular gas consisting primarily H I and H_2 (neutral atomic and molecular hydrogen, respectively). For the exponential disc and central bulge, I employ the results of the Tuorla–Heidelberg study (Flynn et al. 2006), as adapted by McGaugh (2008). The Tuorla–Heidelberg study encompasses a detailed measurement and modeling of the mass-to-light ratio for the Milky Way, resulting in a surface density function of the galactic disc. Using the Tuorla–Heidelberg surface density model, I develop a volumetric density model and a total disc mass model as a function of galactocentric radius. The surface density of the disc is defined as the mass per square kiloparsec of galactic disc stars, treating the galaxy as a flat plate of variable density (the Tuorla–Heidelberg "flat plate" method is standard among studies of the galactic mass distribution). That is, the surface density, in effect, is the integral of the (true) volumetric mass density of the galaxy over the thickness of the disc, yielding a figure with units of mass per unit area. McGaugh makes use of the Tuorla–Heidelberg and other results to develop a detailed mathematical model of the galaxy's disc and bulge density distributions, then employs these models in an application of the theory of modified Newtonian dynamics (MOND) to the galaxy. MOND is an alternative to the dark matter explanation for the apparent "missing mass" of galaxies. McGaugh's presentation of the Tuorla–Heidelberg study results in a disc and bulge mass model of the galaxy that is consistent with known data regarding the surface density of the disc at the solar radius (i.e. the radius of our solar system's orbit about the galactic center), as well as the overall (global) luminosity of the galaxy. Thus, the disc may be assumed to be essentially flat in the surface density equation. To the Tuorla–Heidelberg model, I add the distribution of interstellar gas; based on the data from the study by Olling & Merrifield (2001), I derive a density function for the atomic and molecular hydrogen distribution. Note: for all of the equations given in this Section, masses are expressed in units of solar masses ($M_\odot$), while all distances are in units of kiloparsecs (kpc).

2.1 The Milky Way's exponential stellar disc

Consistent with McGaugh (2008), I adopt a stellar disc distribution as a function of galactocentric radius R according to the following formula:

$$\Sigma_{\text{disc}}(R) = \Sigma_0 e^{-R/R_{\text{d}}}, \tag{3}$$

where R_{d} denotes the scale length, a value of a galactocentric radius by which to scale this exponential function. In order to be consistent with accurate and up-to-date experimental data, I have used a value of 2.5 kpc for R_{d}, consistent with the L-band data from the *COBE* satellite (Binney, Gerhard & Spergel 1997). The L-band is an infrared window: a narrow range of infrared radiation at approximately 3.5 μm for which Earth's atmosphere is fairly transparent. Further, for consistency with the Turola–Heidelberg model (Flynn et al. 2006), I use a value for Σ_0 of 960 $M_\odot$ pc^{-2} from table 1 in McGaugh (2008), equivalent to 9.60×10^8 $M_\odot$ kpc^{-2}.

From Equation 3, I compute two other formulae for use in calculations. First, I convert the function for the surface density of the disc to a three-dimensional volumetric density as a function of radius. In

effect, the galaxy will no longer be treated as a flat plane of stars, but will be assumed for calculational purposes to be a spherically symmetric body. This normalization is accomplished by the following procedure, which may be visualized geometrically. The differential mass contained within a disc band of width dR at radius R is $dM = 2\pi R dR \times \Sigma_{\rm disc}(R)$. However, we wish to compute the differential mass as a function of the equivalent volumetric density by spreading dM over the spherical shell of radius R and thickness dR. Hence, $dM = 4\pi R^2 dR \times \rho_{\rm disc}(R)$. Thus, by equating the previous two expressions for the differential mass, the equation for the volumetric density of the disc is obtained:

$$\rho_{\rm disc}(R) = \frac{1}{2R}\Sigma_{\rm disc}(R) = \frac{1}{2R}\Sigma_0 e^{-R/R_{\rm d}}. \tag{4}$$

Furthermore, to compute the total mass of the disc interior to a galactocentric radius, I integrate Equation 3 to yield:

$$M_{\rm disc}(R) = 2\pi\Sigma_0 \int_0^R r e^{-r/R_{\rm d}} dr = 2\pi\Sigma_0 R_{\rm d}^2 \left[1 - e^{-R/R_{\rm d}}\left(1 + \frac{R}{R_{\rm d}}\right)\right]. \tag{5}$$

2.2 The central bulge

The Milky Way is classified as a barred spiral galaxy, meaning that rather than being perfectly radially symmetric, it has a boxy bulge of stars running through the middle. However, for the purposes of determining the large-scale mass distribution of the galaxy, this treatment will neglect the triaxial nature of the central region, replacing it with an equivalent radially symmetric distribution. Thus, I model the central bulge of the galaxy by normalizing the following formula, as shown by Binney et al. (1997) and utilized in McGaugh's adaptation (2008):

$$\rho_{\rm bulge}(b) = \frac{\rho_{\rm bulge,0}}{\eta\zeta b_{\rm m}^3} \frac{\exp\left[-(b/b_{\rm m})^2\right]}{(1 + b/b_0)^{1.8}}, \tag{6}$$

with $b_{\rm m} = 1.9$ kpc, $b_0 = 0.1$ kpc, $\eta = 0.5$, and $\zeta = 0.6$. In this equation, b is a radial parameter, with $b^2 = x^2 + \eta^{-2}y^2 + \zeta^{-2}z^2$, while $b_{\rm m}$ and b_0 are scaling parameters (analogous to the scale length discussed above for the disc). Because of the galaxy's triaxial boxy bulge, the density is not truly isotropic in R, the true radius, but may be expressed as isotropic in a new radial parameter, b, which is defined by scaling y and z by numerical factors η and ζ. In this way, η and ζ parameterize the extent of the anisotropic nature of the central bulge, i.e. how "boxy" it is. I normalize Equation 6 using the recommendation from McGaugh (2008): for consistency with the model of Bissantz, Englmaier & Gerhard (2003), I substitute R for b with no geometric scaling by $(\eta\zeta)^{1/3}$. This modification yields a softer bulge, with a density profile that drops off somewhat less steeply, with density equation:

$$\rho_{\rm bulge}(R) = \frac{\rho_{\rm bulge,0}}{\eta\zeta b_{\rm m}^3} \frac{\exp\left[-(R/b_{\rm m})^2\right]}{(1 + R/b_0)^{1.8}}. \tag{7}$$

In Equations 6 and 7, I calculate the quantity $\rho_{\rm bulge,0} = 8.97 \times 10^{10}\ {\rm M}_\odot$ from $M_{\rm bulge} = 1.10 \times 10^{10}\ {\rm M}_\odot$ for a choice of scale length of 2.5 kpc, based on the stipulations of the Tuorla–Heidelberg model (Flynn et al. 2006) as expressed by McGaugh (2008). One further note with regard to the bulge density function is that it is not analytically integrable, so to find $M_{\rm bulge}(R)$, the total mass of the bulge interior to a radius, I use numerical integration of the form:

$$M_{\rm bulge}(R) = 4\pi \int_0^R r^2 \rho_{\rm bulge}(r) dr. \tag{8}$$

2.3 The galactic gas distribution

To find the gas distribution within the galaxy, I use the data found in table D1 of the study by Olling & Merrifield (2001), which provides disc surface densities of atomic and molecular hydrogen gas (H I and H_2, respectively) at specific galactocentric radii scaled by R_0, the galactocentric radius of the Sun's orbit. By surface density, we are again using the convention of treating the galaxy as a flat disc. That is, the surface density at a given location denotes the differential mass of gas in a column of disc surface area dA, spanning the thickness of the galactic plane. (We will shortly convert this to a usual volumetric density, as was done for the stellar disc component.) For consistency with the velocity data in Section 3 of this paper, I use $R_0 = 8.5$ kpc, though the choice of R_0 should not greatly affect the final result of this work, since the gas comprises a relatively small fraction of the mass and the potential error in R_0 is comparatively small. In Olling & Merrifield's data, an additional $1.4\,M_\odot\,pc^{-2}$ of ionized gas is included at the solar radius, but at no other galactocentric radius. As suggested by McGaugh (2008), I subtract this 1.4 $M_\odot$ pc^{-2} from the value of the gas surface density at the solar radius, so that all data points uniformly measure only nonionized gas; this also allows for consistency with studies of other galaxies. Furthermore, as McGaugh suggests in his study, I multiply the sum of the atomic and molecular hydrogen components by 1.4 to accommodate the additional masses of heavier elements such as helium and the metals. I then plot the resulting data of surface density as a function of galactocentric radius and specify a best-fitting cubic polynomial passing through the origin (see Fig. 1). The surface density is defined to be zero at $R > 23.521$ kpc, to avoid nonphysical negative densities.

The gas distribution is thus given by the following formula (see Table 1 for constants G_i):

$$\Sigma_{\text{gas}}(R) = \begin{cases} \sum_{i=1}^{3} G_i R^i & R \leq 23.521 \text{ kpc} \\ 0 & R > 23.521 \text{ kpc} \end{cases}. \tag{9}$$

Similarly to the exponential disc distribution, this zone of gas can be normalized to a three-dimensional density function of radius, averaged over the entire sphere:

$$\rho_{\text{gas}}(R) = \frac{1}{2R}\Sigma_{\text{gas}}(R) = \begin{cases} \sum_{i=1}^{3} \frac{G_i}{2} R^{i-1} & R \leq 23.521 \text{ kpc} \\ 0 & R > 23.521 \text{ kpc} \end{cases}. \tag{10}$$

Also, as in the case of the exponential disc, I computed the function $M_{\text{gas}}(R)$, the total gas interior to a radius, via integration (see Table 1 for constants H_i):

$$M_{\text{gas}}(R) = 2\pi \int_0^R r\Sigma_{\text{gas}}(r)dr = \begin{cases} \sum_{i=3}^{5} H_i R^i & R \leq 23.521 \text{ kpc} \\ H_6 & R > 23.521 \text{ kpc} \end{cases}. \tag{11}$$

Table 1: Constants for model of galactic gas distribution.

i	G_i	H_i
1	2.7915×10^6	
2	-1.963×10^5	
3	3.3×10^3	5846503.92833
4		-308347.31895
5		4146.90230274
6		11556424162.9

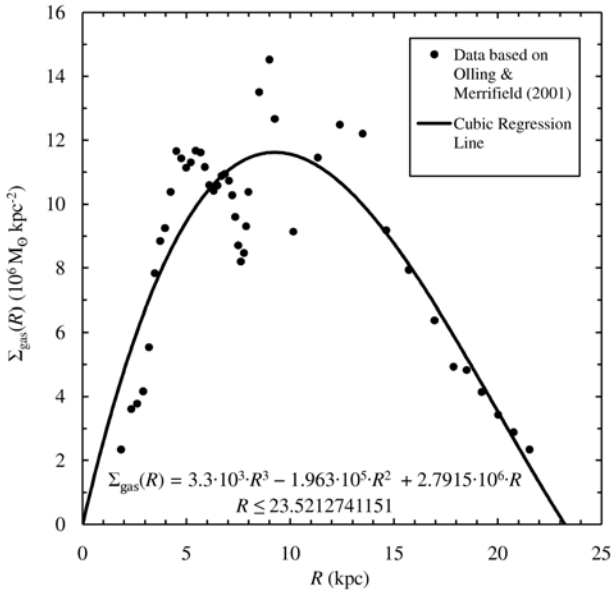

Figure 1: Total atomic and molecular gas surface density of the galaxy, based on the data from Olling & Merrifield (2001), along with the best-fitting cubic polynomial passing through the origin.

2.4 Total baryonic mass distribution

Thus, by summing the various components of baryonic matter, including luminous matter in stars as well as interstellar gas, the total distribution of the baryonic mass of the galaxy may be expressed. Specifically, the three-dimensional volumetric density of galactic baryonic matter may be formulated locally as a single explicit function:

$$\rho_{\text{model}}(R) = \rho_{\text{disc}}(R) + \rho_{\text{bulge}}(R) + \rho_{\text{gas}}(R). \tag{12}$$

Similarly, the total baryonic mass interior to a galactocentric radius may be expressed as:

$$M_{\text{model}}(R) = M_{\text{disc}}(R) + M_{\text{bulge}}(R) + M_{\text{gas}}(R). \tag{13}$$

See Fig. 2 for a visual summary of the galactic mass model and its components.

3 The Rotational Velocity Curve of the Galaxy

The rotational velocity curve of the Milky Way has been notoriously difficult to determine. Years of astronomical observation and multiple studies have been devoted to this task. While the velocity of the region interior to the solar radius is more accurately known, the curve at large distances is much less definite. For the present study, I use the function produced in the Massachusetts-Stony Brook galactic plane CO survey (Clemens 1985) for the velocity curve interior to 8.5 kpc. For the velocity curve at galactocentric radii greater than 8.5 kpc, I derive an exponential function based on the recent data from the study of the SDSS Blue Horizontal-Branch (BHB) stars by Xue et al. (2008). Together, these two studies, along with my calculations, provide a rotation curve of the galaxy at galactocentric radii of up to 55 kpc that is consistent with the best data at the present date. Note: all velocity functions $V(R)$ defined in this Section provide values in units of kilometers per second, where the

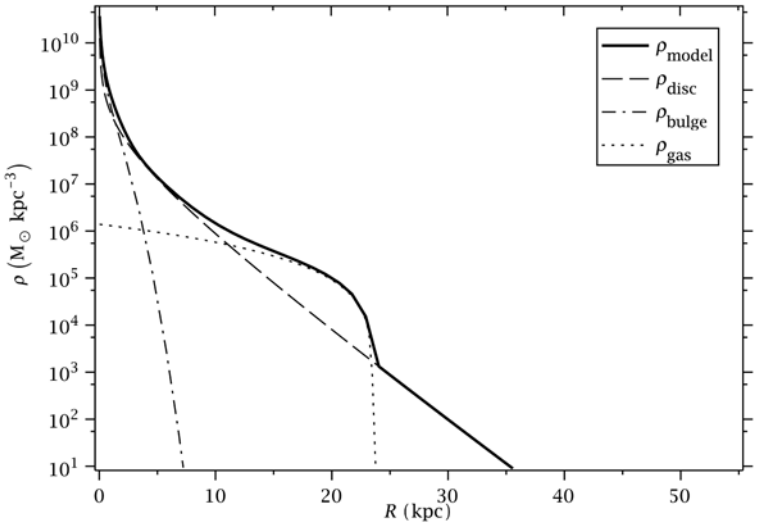

Figure 2: Summary of the mass model of the galaxy, with the three-dimensional volumetric density of each component and the total plotted as a function of galactocentric radius.

value of R is in kiloparsecs.

3.1 The rotation curve interior to 8.5 kpc

The Massachusetts-Stony Brook galactic plane CO survey provides quite precise data for radii interior to 8.5 kpc (see their fig. 3). Clemens incorporates data from not only the CO survey, but also H I, H II, and CO data from other sources. However, the error in the data from Clemens (1985) becomes alarmingly large at radii greater than 8.5 kpc. Thus, I use the best-fitting piecewise polynomial produced by Clemens (1985) for $R < 8.5$ kpc (see Fig. 3 for illustration and Table 2 for constants):

$$V(R) = \begin{cases} \sum_{i=0}^{6} A_{1,i} R^i & R < 0.765 \text{ kpc} \\ \sum_{i=0}^{5} A_{2,i} R^i & 0.765 \text{ kpc} \leq R < 3.825 \text{ kpc} \\ \sum_{i=0}^{7} A_{3,i} R^i & 3.825 \text{ kpc} \leq R < 8.5 \text{ kpc} \end{cases} . \tag{14}$$

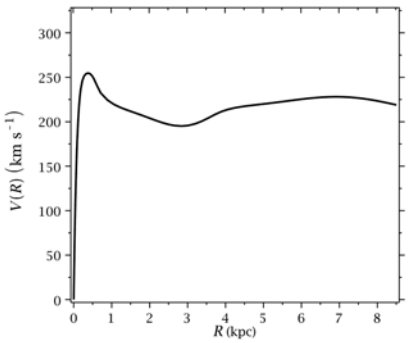

Figure 3: The rotational velocity curve interior to 8.5 kpc, as defined by Equation 14. This function is from the Massachusetts-Stony Brook galactic plane CO survey (Clemens 1985).

3.2 The rotation curve for large radii

Outside of 8.5 kpc, the radius of the Sun's orbit about the galactic center, the rotation curve is less certain. However, the recent study by Xue et al. (2008) allows for the definition of a fairly accurate curve as far as a galactocentric radius of 55 kpc. Using the data from their table 3, I defined the velocity at $R = 55$ kpc to be $\beta = V(55\,\text{kpc}) = 180$ km s^{-1}, which is consistent with both models that Xue et al. (2008) use to interpret their data. Furthermore, I stipulate that the value and first derivative of the velocity curve at the Sun's orbit of 8.5 kpc match the values previously defined by the piecewise polynomial in Equation 14: $\alpha = V(8.5\,\text{kpc}) = 218.955757463$ km s^{-1} and $\gamma = V'(8.5\,\text{kpc}) = -9.597324992$ km s^{-1} kpc^{-1}. This is done to ensure continuity and differentiability of the new velocity curve, when combined with the results from the Massachusetts-Stony Brook galactic plane CO survey, as given in Equation 14. Thus, with the constants α, β, and γ, I define the following system of equations to solve for an exponential function for the velocity curve at $R > 8.5$ kpc, of the form $V(R) = A_4 e^{A_5 R} + A_6$:

$$\begin{cases} A_4 e^{8.5A_5} + A_6 = \alpha \\ A_4 e^{55A_5} + A_6 = \beta \\ A_4 A_5 e^{8.5A_5} = \gamma \end{cases}. \tag{15}$$

See Table 2 for the solution of this system. Equation 15 incorporates constraints drawn from the data of both Xue et al. and Clemens: the parameter β encompasses the result of Xue et al. (2008), while α and γ preserve smoothness and continuity of the velocity curve with that of Clemens (1985). A point of note is how well the exponential curve I have defined fits both models of the velocity data given by Xue et al. (2008) in their table 3. The model exponential curve I have defined corresponds to both of the data sets of Xue et al. for galactocentric radii greater than 8.5 kpc with a reduced χ^2 value of 0.85, indicating goodness of fit. Taking the error bars into account, the curve passes through the majority of the given entries in both models that Xue et al. use to represent their results. To summarize, as a result of my calculations in this Section, the velocity curve of the galaxy has been extended. It is represented as a piecewise function over a range of galactocentric radii of up to 55 kpc (see Fig. 4):

$$V(R) = \begin{cases} \sum_{i=0}^{6} A_{1,i} R^i & R < 0.765\,\text{kpc} \\ \sum_{i=0}^{5} A_{2,i} R^i & 0.765\,\text{kpc} \le R < 3.825\,\text{kpc} \\ \sum_{i=0}^{7} A_{3,i} R^i & 3.825\,\text{kpc} \le R < 8.5\,\text{kpc} \\ A_4 e^{A_5 R} + A_6 & 8.5\,\text{kpc} \le R < 55\,\text{kpc} \end{cases}. \tag{16}$$

4 Results: Calculation of the Galactic Dark Matter Distribution

4.1 Calculation of the total galactic mass distribution

Using Equations 1 and 16, along with the definitions above, one may readily find that the total mass interior to a galactocentric radius is given by the following function (see Table 3 for the new constants and Fig. 5 for illustration):

$$M_V(R) = \begin{cases} \sum_{i=3}^{13} B_{1,i} R^i & R < 0.765\,\text{kpc} \\ \sum_{i=1}^{11} B_{2,i} R^i & 0.765\,\text{kpc} \le R < 3.825\,\text{kpc} \\ \sum_{i=1}^{15} B_{3,i} R^i & 3.825\,\text{kpc} \le R < 8.5\,\text{kpc} \\ R\left(B_4 + B_5 e^{A_5 R} + B_6 e^{2A_5 R}\right) & 8.5\,\text{kpc} \le R < 55\,\text{kpc} \end{cases}. \tag{17}$$

Furthermore, if $\rho_V(R)$ is defined as the total local three-dimensional volumetric density of all galac-

Table 2: Constants for the galactic rotational velocity function $V(R)$.

i	$A_{1,i}$	$A_{2,i}$	$A_{3,i}$
0	0	325.0912	−2342.6564
1	3069.81	−248.1467	2507.60391
2	−15809.8	231.87099	−1024.068760
3	43980.1	−110.73531	224.562732
4	−68287.3	25.073006	−28.4080026
5	54904	−2.110625	2.0697271
6	−17731		−0.08050808
7			0.00129348

A_4	A_5	A_6
316.244380231	−0.246362129903	179.999587553

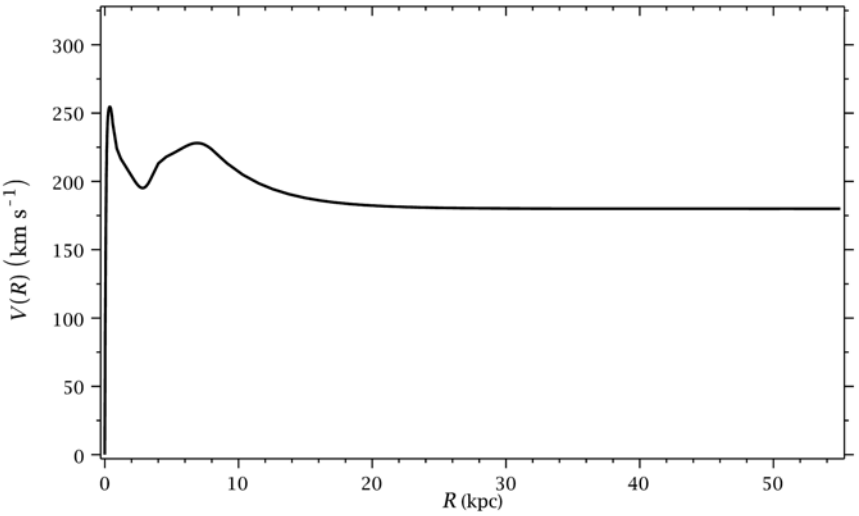

Figure 4: The full rotational velocity curve of the galaxy (Equation 16).

tic matter as a function of radius, as calculated from the velocity curve, then assuming a spherically symmetric mass distribution:

$$M_V(R) = 4\pi \int_0^R r^2 \rho_V(r) dr. \tag{18}$$

Equivalently,

$$\rho_V(R) = \frac{1}{4\pi R^2}\frac{d}{dR}\left(M_V(R)\right)$$
$$= \begin{cases} \sum_{i=0}^{10} C_{1,i} R^i & R < 0.765 \text{ kpc} \\ \sum_{i=-2}^{8} C_{2,i} R^i & 0.765 \text{ kpc} \leq R < 3.825 \text{ kpc} \\ \sum_{i=-2}^{12} C_{3,i} R^i & 3.825 \text{ kpc} \leq R < 8.5 \text{ kpc} \\ \frac{1}{4\pi}\left[B_4 R^{-2} + B_5 e^{A_5 R}\left(R^{-2} + A_5 R^{-1}\right) + B_6 e^{2A_5 R}\left(R^{-2} + 2A_5 R^{-1}\right)\right] & 8.5 \text{ kpc} \leq R < 55 \text{ kpc} \end{cases} . \quad (19)$$

Equation 19 is illustrated in Fig. 6. See Table 4 for new constants.

Thus, functions of the total mass distribution of the galaxy may be calculated and inferred from the rotational velocity curve (Equation 16).

Table 3: Constants for the function $M_V(R)$

i	$B_{1,i}$	$B_{2,i}$	$B_{3,i}$
1		24564047744.2	$1.27557704529 \times 10^{12}$
2		-37500168484.2	$-2.73078201846 \times 10^{12}$
3	$2.19034486335 \times 10^{12}$	49352771367.2	$2.57674025074 \times 10^{12}$
4	$-2.25609495184 \times 10^{13}$	-43481386377.7	$-1.43828292011 \times 10^{12}$
5	$1.20856086239 \times 10^{14}$	29059006683.2	536455819305
6	$-4.20670428948 \times 10^{14}$	-15147014255.6	-142270621544
7	$1.02978778528 \times 10^{15}$	5796118507.53	27744819989.6
8	$-1.82490561972 \times 10^{15}$	-1518158230.29	-4046039381.34
9	$2.33664373715 \times 10^{15}$	254764268.883	443464513.413
10	$-2.10536449516 \times 10^{15}$	-24600106.3077	-36352078.8409
11	$1.26349411608 \times 10^{15}$	1035408.34664	2193858.98095
12	$-4.5253973374 \times 10^{14}$		-94540.2910909
13	$7.30728363957 \times 10^{13}$		2750.99016397
14			-48.4081726383
15			0.388874030682

B_4	B_5	B_6
7530651076.8057	26461461549.993	23245299118.903

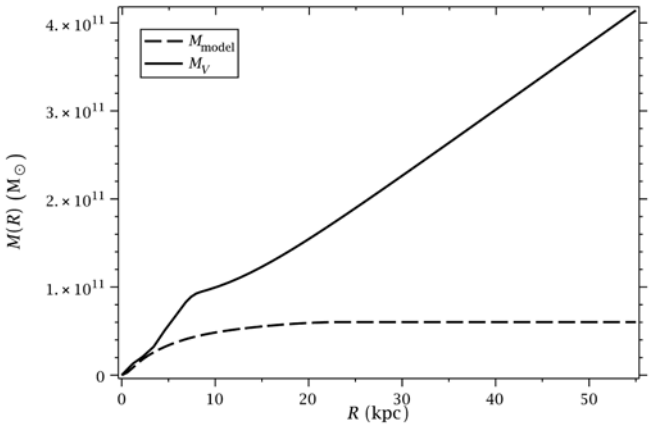

Figure 5: An illustration of the discrepancy between the mass interior to a galactocentric radius as predicted by the velocity curve (M_V), as opposed to the mass accounted for in the galactic mass model ($M_{\rm model}$).

4.2 Calculation of the dark matter distribution

In this Section, I define $\rho_{\rm DM}(R)$, the three-dimensional volumetric density distribution of dark matter, as $\rho_V(R) - \rho_{\rm model}(R)$, and similarly, $M_{\rm DM}(R) = M_V(R) - M_{\rm model}(R)$. Thus, I have calculated the dark matter density distribution of the Milky Way Galaxy, expressed as a single function:

$$\rho_{\rm DM}(R) = \begin{cases} \sum_{i=0}^{10} C_{1,i} R^i & R < 0.765 \text{ kpc} \\ \sum_{i=-2}^{8} C_{2,i} R^i & 0.765 \text{ kpc} \le R < 3.825 \text{ kpc} \\ \sum_{i=-2}^{12} C_{3,i} R^i & 3.825 \text{ kpc} \le R < 8.5 \text{ kpc} \\ \frac{1}{4\pi}\left[B_4 R^{-2} + B_5 e^{A_5 R}\left(R^{-2} + A_5 R^{-1}\right) + B_6 e^{2A_5 R}\left(R^{-2} + 2A_5 R^{-1}\right)\right] & 8.5 \text{ kpc} \le R < 55 \text{ kpc} \end{cases}$$
$$- \left\{ \frac{1}{2R}\Sigma_0 e^{-R/R_{\rm d}} + \frac{\rho_{\rm bulge,0}}{\eta\zeta b_{\rm m}^3} \frac{\exp\left[-\left(R/b_{\rm m}\right)^2\right]}{\left(1 + R/b_0\right)^{1.8}} + \begin{cases} \sum_{i=1}^{3} \frac{G_i}{2} R^{i-1} & R \le 23.521 \text{ kpc} \\ 0 & R > 23.521 \text{ kpc} \end{cases} \right\}. \quad (20)$$

Furthermore, the total mass of dark matter interior to a given galactocentric radius may be expressed by the function:

$$M_{DM}(R) = \begin{cases} \sum_{i=3}^{13} B_{1,i} R^i & R < 0.765 \text{ kpc} \\ \sum_{i=1}^{11} B_{2,i} R^i & 0.765 \text{ kpc} \le R < 3.825 \text{ kpc} \\ \sum_{i=1}^{15} B_{3,i} R^i & 3.825 \text{ kpc} \le R < 8.5 \text{ kpc} \\ R\left(B_4 + B_5 e^{A_5 R} + B_6 e^{2A_5 R}\right) & 8.5 \text{ kpc} \le R < 55 \text{ kpc} \end{cases} - 2\pi\Sigma_0 R_{\rm d}^2 \left[1 - e^{-R/R_{\rm d}}\left(1 + \frac{R}{R_{\rm d}}\right)\right]$$
$$- 4\pi \frac{\rho_{\rm bulge,0}}{\eta\zeta b_{\rm m}^3} \int_0^R r^2 \frac{\exp\left[-\left(r/b_{\rm m}\right)^2\right]}{\left(1 + r/b_0\right)^{1.8}} dr - \begin{cases} \sum_{i=3}^{5} H_i R^i & R \le 23.521 \text{ kpc} \\ H_6 & R > 23.521 \text{ kpc} \end{cases}. \quad (21)$$

These calculations are depicted graphically in Figs. 7, 8, and 9. Note in Fig. 7 that the density of galactic dark matter decreases faster than a density profile $\propto R^{-2}$, since the velocity curve decreases somewhat at large galactocentric radii before leveling off; a density profile proportional to R^{-2} would

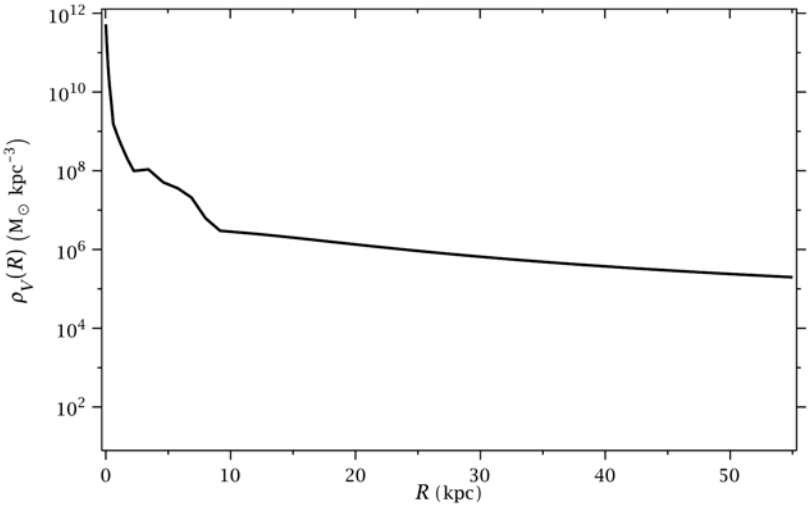

Figure 6: The three-dimensional volumetric density of the total matter in the galaxy as a function of galactocentric radius, based on the rotational velocity curve.

be consistent with a constant rotational velocity. Similarly, in Fig. 8, one may observe that the mass of dark matter interior to a galactocentric radius increases almost linearly with distance. Both of these observations are consistent with the concept of a galaxy dominated by dark matter, especially at large radii, a hypothesis supported by Fig. 9.

A further item of note is the irregular behavior of the predicted density of dark matter at galactocentric radii smaller than approximately 2.5 to 3 kpc. Within this region, the dark matter density curve behaves anomalously, predicting negative values, then reaching high positive densities near the very center of the galaxy. These odd effects are explained, however, by the complex nature of the galactic center. The mass model I use is radially symmetric, while in fact the galaxy has a triaxial, boxy bulge at the center, leading to noncircular orbital motions and the destruction of the radial symmetry of the velocity curve. Thus, the supposed negative density of dark matter interior to 3 kpc is simply due to the fact that matter at this radius is rotating more slowly than what would be expected from the mass model. Likewise, the unexpectedly high predicted dark matter density values near the galactic center simply denote the fact that matter at the very center of the galaxy rotates faster than what would be expected from the observable matter, possibly a consequence of the supermassive central black hole. For clarity, the anomalous values in the center of the galaxy have been truncated from the graphs in Figs. 7 through 9.

Overall, the velocity data demand that a total mass of approximately 4.14×10^{11} $M_\odot$ is contained within a galactocentric radius of 55 kpc. However, the mass model only accounts for a mass of approximately 6.03×10^{10} $M_\odot$ inside this radius. Thus, of the total mass of the galaxy interior to a 55 kpc radius, approximately 14.5 percent is contained in observable baryonic matter, while the remaining 85.5 percent is dark matter (see Fig. 9). The dark matter halo of the Milky Way thus has a mass interior to 55 kpc of approximately 3.54×10^{11} $M_\odot$. The extent to which this halo extends beyond 55 kpc is unclear, but it is evident from these calculations that dark matter dominates the composition of the galaxy. This study thus provides significant new insight into the distribution of galactic dark matter, while quantitatively confirming at the local galactic level the generally accepted belief that dark matter is the main component of matter in the universe as a whole.

A further intriguing calculation involves the comparison of the density of galactic dark matter to the overall average dark matter density of the universe. Using the value provided by Fukugita & Peebles (2004), the energy density of dark matter in the universe is: $\Omega_{\mathrm{DM}} = 0.23$, or alternatively,

Table 4: Constants for the function $\rho_V(R)$

i	$C_{1,i}$	$C_{2,i}$	$C_{3,i}$
-2		1954744810.42	101507196026
-1		-5968337181.04	-434617456744
0	522906318117	11782106277.6	615151421954
1	$-7.1813732734 \times 10^{12}$	-13840555149	-457819672600
2	$4.80871088192 \times 10^{13}$	11562211387.4	213448988482
3	$-2.00855334539 \times 10^{14}$	-7232166575.59	-67929218026.5
4	$5.7363535727 \times 10^{14}$	3228683189.27	15455038362.9
5	$-1.16177100022 \times 10^{15}$	-966489546.985	-2575788669.94
6	$1.67349780455 \times 10^{15}$	182461467.222	317608062.28
7	$-1.67539583207 \times 10^{15}$	-19576142.5973	-28928065.196
8	$1.10600233778 \times 10^{15}$	906346.960675	1920399.25696
9	$-4.32143613421 \times 10^{14}$		-90279.3278908
10	$7.55943702678 \times 10^{13}$		2845.91893945
11			-53.93079973
12			0.464184181673

$\rho_{\rm DM} = 0.23\rho_{\rm c0}$, where the density parameter $\Omega = 1$, meaning that the density of the universe in the present epoch equals the present critical density, given by Binney & Tremaine (2008) as $\rho_{\rm c0} = 1.3599{\times}10^5 {\rm M}_\odot\ {\rm kpc}^{-3}$, assuming consistently with Fukugita & Peebles (2004) that the Hubble constant is exactly 70 km s^{-1} Mpc^{-1}. Thus, $\rho_{\rm DM} = 3.1278 \times 10^4\ {\rm M}_\odot\ {\rm kpc}^{-3}$, a value that is significantly lower than the density of dark matter within a galactocentric radius of 55 kpc, though comparable to the galactic dark matter density at large radii (see Table 5 for specific values). Therefore, as compared to the universe as a whole, the galaxy is a relatively compact object, but not excessively dense.

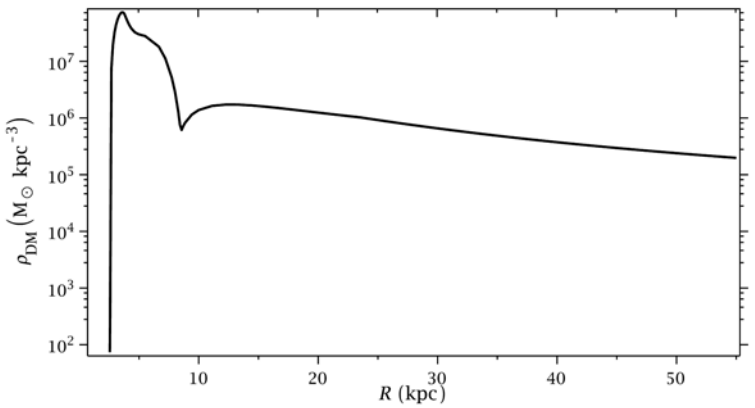

Figure 7: The density of dark matter in the Milky Way Galaxy as a function of galactocentric radius (Equation 20). Note the gradual decline of the density curve at large radii (see Table 5).

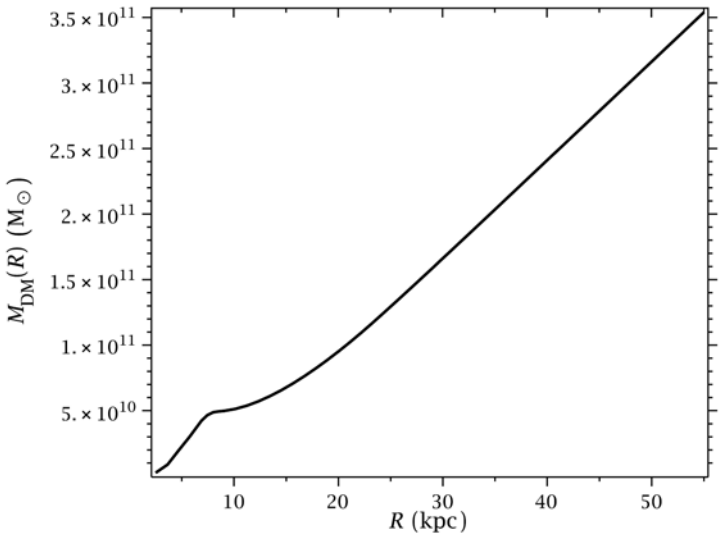

Figure 8: The total mass of dark matter interior to a galactocentric radius. Note the linearity of the function at great distances from the galactic center, implying the domination of dark matter.

5 The Role of Neutrinos

Neutrinos have often been proposed as a component of dark matter and therefore are of interest in an examination of the effects of dark matter within the galaxy. Long thought to be massless, relatively recent experiments have proven that neutrinos do, in fact, possess a small mass. Thus, neutrinos create a gravitational effect. In this Section, I estimate the validity of the proposition of neutrinos as candidate dark matter particles within the Milky Way Galaxy.

There exist three types, or flavors, of neutrinos, and experiments have not yet been able to determine the specific mass of any particular flavor. However, the sum of the masses of the three flavors has been estimated using cosmological constraints not to exceed 0.3 eV (Goobar et al. 2006).

To calculate the gravitational effect of neutrinos, one must initially determine the density of neutrinos within the galaxy. To astrophysical accuracy, one can show that the density of neutrinos throughout space can be approximated as a constant. This can be understood by considering the energy of a single neutrino of average energy from the Cosmic Neutrino Background (CνB), the inundation of neutrinos left over from the Big Bang that fills all of space, similar to the Cosmic Microwave Background (CMB). By treating neutrinos as relativistic radiation particles, which is a common method used in this type of calculation, one can show that the effective temperature of the CνB is given by:

$$T_\nu = \left(\frac{4}{11}\right)^{1/3} T_\gamma, \tag{22}$$

where T_γ is the temperature of the CMB (Mangano et al. 2008). Using a value of $T_\gamma = 2.725$ K (Fixsen & Mather 2002), Equation 22 yields a value of $T_\nu = 1.945$ K. Thus, one can assert that the energy of the neutrino is:

$$E_\nu = \frac{3}{2} k T_\nu = 2.514 \times 10^{-4}\,\text{eV}, \tag{23}$$

using the latest (2006) value of Boltzmann's constant, $k = 1.3806504 \times 10^{-23}$ J K^{-1}, and the electron volt, $1.602176487 \times 10^{-19}$ J, given by CODATA and NIST (Mohr et al. 2007).

However, one can also compute the gravitational potential energy difference that the neutrino

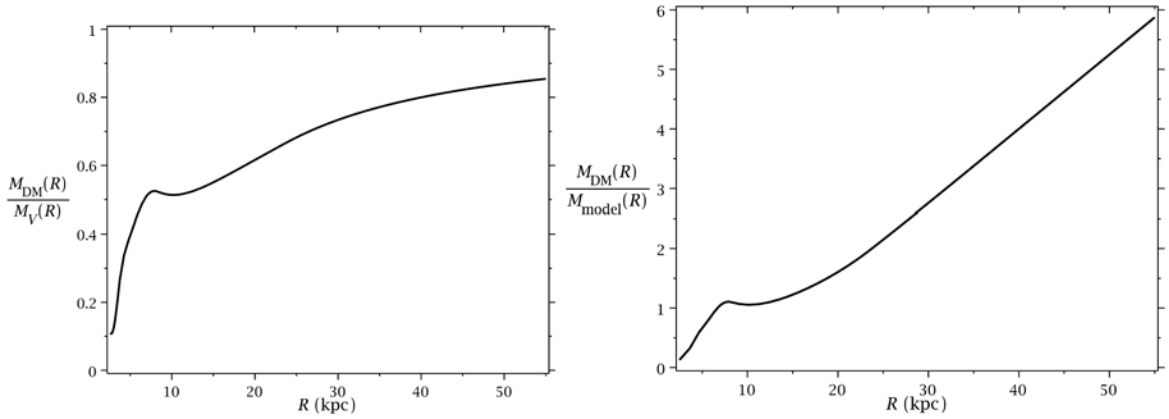

Figure 9: (left) The ratio of dark matter to total matter in the galaxy. Note that the curve levels off somewhat as the dark matter density decreases, reaching a value of about 85 percent dark matter interior to 55 kpc. (right) The ratio of dark matter to baryonic matter, illustrating the dominance of dark to baryonic components in the composition of the Milky Way.

gains as it falls from deep space (essentially, an infinite distance) towards the center of the galaxy, taking into account only the galactic mass within the radius of 55 kpc. Since the masses of the three flavors of neutrinos are not known, this average neutrino will be taken to possess a mass of one third the total mass, or $m_\nu = 0.1$ eV (which is equivalent to 1.783×10^{-37} kg). Thus, the gravitational potential energy difference is given by:

$$\Delta U = 4\pi G m_\nu \int_0^{55} \frac{\rho_V(r) r^2}{r} dr = 6.204 \times 10^{-26} \text{ J} = 3.872 \times 10^{-7} \text{ eV}. \tag{24}$$

As one can see, $\Delta U \ll E_\nu$, so any kinetic energy that the neutrino gains in falling toward the Milky Way is negligible compared to the energy that the neutrino possesses as a result of its temperature, by Equation 23. Thus, the neutrino is not bound to the galaxy and its orbit has a large positive total energy, indicating that the gravitational effect of the galaxy has only a small effect on the distribution of cosmic neutrinos. Therefore, for the purposes of this study, the neutrino density can be asserted to be constant.

As shown by Lopez et al. (1999) and Mangano et al. (2008), the energy density of cosmic neutrinos and photons are related by the equation:

$$\rho_\nu = \frac{7}{8}\left(\frac{4}{11}\right)^{4/3} N_\nu \rho_\gamma, \tag{25}$$

where N_ν is the effective number of neutrinos. When oscillations between the three flavors of massive neutrinos are taken into account, $N_\nu = 3.046$ (Mangano et al. 2008).

Since the CMB radiation can be treated as that of a blackbody, the energy density of the CMB may be found thus:

$$\rho_\gamma = \frac{4\sigma T_\gamma^4}{c} = 4.172 \times 10^{-14} \text{ J m}^{-3}. \tag{26}$$

Thus, $\rho_\nu = 2.886 \times 10^{-14}$ J m^{-3}. Here, the value of the Stefan-Boltzmann constant σ is the CODATA (2006) value of 5.670400×10^{-8} W m^{-2} K^{-4} (Mohr et al. 2007). The speed of light is the defined value of 299792458 m s^{-1}.

Using this neutrino energy density, along with the energy of our single average neutrino (Equation

Table 5: Selected values of the predicted density of galactic dark matter at various radii (Equation 20).

R (kpc)	ρ_{DM} ($\mathrm{M}_\odot\ \mathrm{kpc}^{-3}$)
3	3.7139×10^7
5	2.9909×10^7
8	2.9630×10^6
8.5	5.6253×10^5
10	1.3843×10^6
12	1.7183×10^6
15	1.6304×10^6
20	1.2454×10^6
25	9.2106×10^5
30	6.5652×10^5
35	4.8683×10^5
40	3.7393×10^5
45	2.9578×10^5
50	2.3967×10^5
55	1.9809×10^5

23), one may find the number density of neutrinos:

$$n_\nu = \frac{\rho_\nu}{E_\nu} = 7.164 \times 10^8\ \mathrm{m}^{-3}, \tag{27}$$

which can readily be converted into a mass density:

$$\mu_\nu = m_\nu n_\nu = 1.277 \times 10^{-28}\ \mathrm{kg\,m}^{-3} = 1.886\ \mathrm{M}_\odot\ \mathrm{kpc}^{-3}. \tag{28}$$

The neutrino densities calculated in this Section are consistent with the results of Fukugita & Peebles (2004), taking into account the uncertainty inherent in the neutrino mass estimate.

As one can see by comparison with the values of the predicted dark matter density in Fig. 7, neutrinos can only comprise a very small fraction of galactic dark matter and do not nearly account for the observed quantities of dark matter present in the galaxy.

6 Conclusions

The observed mass and the observed rotational velocity curve of the Milky Way Galaxy are seemingly inconsistent without the addition of dark matter. As I have shown, the galaxy's rotational velocity levels off at large distances, rather than falling in the characteristic Keplerian fashion, implying the existence of large quantities of invisible dark matter.

Through the development of a mass model of the galaxy and an analysis of the rotational velocity curve, I have been able to produce an estimate of the dark matter content of the Milky Way. Interior to a galactocentric radius of 55 kpc, the $\sim 4 \times 10^{11}$ $\mathrm{M}_\odot$ of matter in our galaxy is roughly 85 percent dark (or approximately 3.5×10^{11} $\mathrm{M}_\odot$ is dark matter). The results of this study provide a new and detailed glimpse into the dark matter structure of the galaxy, while maintaining consistency with conventional astrophysical theory on the subject, which holds that dark matter makes up the majority of all matter in the universe.

The galactic mass model employed followed mainly from the Tuorla–Heidelberg model (Flynn et al. 2006), with an exponential stellar disc and central stellar bulge. In addition, the model incorporated my calculation of the distribution of gas in the galaxy, from data supplied by Olling & Merrifield

(2001). The data for the velocity curve consisted of two main parts: the inner curve is represented as a piecewise function from the Massachusetts-Stony brook CO survey (Clemens 1985), while the outer rotation curve is a function I derived based on data from the study by Xue et al. (2008).

More importantly, I have been able to quantitatively determine the distribution of dark matter within our galaxy. This distribution follows a pattern roughly inversely proportional to the square of the galactocentric radius, but the curve contains some interesting complexities that may serve as grounds for future study in this area. The results of this study are relevant for any experiment or theoretical discussion involving the dark matter content of the galaxy. In experimental investigation, a knowledge of the local dark matter density is conducive to decisive detection of particles proposed as dark matter candidates. In the theoretical realm, the dark matter distribution could lend insight into the dynamics of galaxy formation and evolution.

Finally, through a discussion of the properties of neutrinos and various calculations, I demonstrated that, given the data from the Cosmic Neutrino Background, as well as current constraints on neutrino mass, neutrinos can only account for a small component of the dark matter necessary to create the rotation of the galaxy. The search for the true nature of dark matter continues, broadening our understanding of the fundamental nature of the universe.

Acknowledgments

I would like to thank my research mentor, Dr. Thomas Walsh, of the University of Minnesota, for all of his constructive advice. I am further thankful for helpful communication with Dr. Stacy S. McGaugh of the University of Maryland.

References

[1] Binney J., Tremaine S., 1987, Galactic Dynamics. Princeton Univ. Press, Princeton, NJ

[2] Binney J., Tremaine S., 2008, Galactic Dynamics, Second Ed. Princeton Univ. Press, Princeton, NJ

[3] Binney J., Gerhard O., Spergel D., 1997, MNRAS, **288**, 365

[4] Bissantz N., Englmaier P., Gerhard O., 2003, MNRAS, **340**, 949-968

[5] Clemens D. P., 1985, ApJ, **295**, 422-436

[6] Fixsen D. J., Mather, J. C., 2002, ApJ, **581**, 817-822

[7] Flynn C., Holmberg J., Portinari L., Fuchs B., Jahreiß H., 2006, MNRAS, **372**, 1149-1160

[8] Fukugita M., Peebles, P. J. E., 2004, ApJ, **616**, 643-668

[9] Goobar A., Hannestad S., Mörtsell E., Tu H., 2006, J. Cosmol. Astropart. Phys., JCAP **06** (2006) 019

[10] Lopez R. E., Dodelson S., Heckler A., Turner M. S., 1999, Phys. Rev. Lett., **82**, 3952-3955

[11] McGaugh S. S., 2008, ApJ, **683**, 137-148

[12] Mangano G., Miele G., Pastor S., Pinto T., Pisanti O., Serpico P. D., 2005, Nucl. Phys. B,**729**, 221-234

[13] Mohr P. J., Taylor B. N., Newell D. B., 2007, CODATA Recommended Values of the Fundamental Physical Constants: 2006. NIST, Gaithersburg, MD

[14] Olling R. P., Merrifield M. R., 2001, MNRAS, **326**, 164-180

[15] Seidelmann P. K., United States Naval Observatory 2005, Explanatory Supplement to the Astronomical Almanac. University Science Books, Nautical Almanac Office, Great Britain

[16] Williams D. R., 2004, Sun Fact Sheet. NASA Goddard Space Flight Center, Greenbelt, MD

[17] Xue X.-X., Rix H.-W., Zhao G. et al. 2008, ApJ, **684**, 1143-1158